 https://doi.org/10.3311/PPci.20508

Periodica Polytechnica Civil Engineering, 66(4), pp. 1048–1059, 2022

A Framework for Optimization of Double Layer Grids with Supporting Cables

Ali Kaveh[1*], Milad Akbari[1]

[1] School of Civil Engineering, Iran University of Science and Technology, Narmak, Tehran, Postal Code 16846-13114, Iran
[*] Corresponding author, e-mail: alikaveh@iust.ac.ir

Received: 22 May 2022, Accepted: 26 June 2022, Published online: 07 July 2022

Abstract

Space structures are used when it is required to cover a large unpaved area such as sports stadiums, aircraft factories, bridges, etc. Weight minimization is important in optimizing space structures, having various advantages such as cost reduction, reduction of the deterioration, increasing the possibility of using larger spans, and easy transportation and installation process. The use of meta-heuristic algorithms, inspired by the physics laws of nature, allows us to optimize a variety of complex problems. In this paper, four structures with different spans with and without cables are examined. Optimization is performed using Enhanced Colliding Bodies Optimization (ECBO) and Vibrating Particles System (VPS) optimization algorithms. The optimization is aimed to minimize the weight and the mid-span deflection of the structures. The utilized methods are based on the optimization algorithms in MATLAB (MATrix LABoratory) programming and the SAP2000 (Structural Analysis Program 2000) finite element software. In this way, the results, obtained from the structural analysis in finite element software, are utilized by the optimization algorithms and the operation is repeated until the optimal weight is achieved. In all the investigated examples, the ECBO performed better than the VPS algorithm. The findings indicate that the addition of the cables, in addition of reducing the weight of the structures can reduce the mid-span deflection.

Keywords

optimization, meta-heuristic algorithms, double layer grids, cables

1 Introduction

Structural optimization is a challenging issue, recently attracted the attention of engineers and researchers, since an optimized structure can have the best performance in terms of stability, economic issues, as well as ease and speed of implementation [1–3]. In recent years, new structural optimization methods have been introduced, have been used in various studies such as optimization of space structures [4–5]. Space structures are very important because of providing architectural spaces and covering large spaces such as swimming pools, train stations, airport lounges, aircraft hangars, sports stadiums, etc. [6–7]. Due to the fact that the three-dimensional performance of the space structures leads to bearing capacity in all directions and reduces the dead weight of the structure, compared to traditional systems, the space structures are relatively light and at the same time have considerable rigidity [8]. In addition, lattice space structures often show good resistance to progressive chain rupture due to the existence of secondary load transfer paths [9]. Especially in the case of space structures in which the architectural function requires that free and relatively large openings be provided in two orthogonal directions in the plan, traditional structures consisting of beams and one-way trusses in such applications, are considered an unfavorable structure from technical and economic aspects and from the point of view of stability and structural behavior on the one hand and dead weight on the other hand, by using such structures, functional, safety and economic intentions will not be satisfactorily met [10]. So, the use of space structures with a suitable form to increase rigidity, increase safety and stability, improve reliability and lighten dead weight, increases free openings and at the same time saves materials and destroys the environment less [11–12]. Large spatial space structures are of two groups: (1) the first group is based on light weight and high strength of materials such as steel cables and membranes; (2) and the second group is based on the

Cite this article as: Kaveh, A., Akbari, M. "A Framework for Optimization of Double Layer Grids with Supporting Cables", Periodica Polytechnica Civil Engineering, 66(4), pp. 1048–1059, 2022. https://doi.org/10.3311/PPci.20508

combination of different structural forms and materials such as cable-stayed structures, composite space trusses, reinforced structures, polygonal space structures, etc. [13].

Large-span space structures still need to be improved in design and construction technology, and many more varieties of them will be developed in the future. The use of double-layer grid as a roof is a suitable solution for covering large areas without columns, but due to the large dimensions as well as the large number of nodes and elements, the use of this type of space structures must be economically justified. Therefore, optimization in the design of space structures is considered very important. In previous studies, the maximum dimensions of optimised two-layer grids were 40 × 40 m^2 [14]. And regarding the restraint of structures, the use of cable to reduce the weight of the grid and the mid-span deflection was not investigated [15–17]. Also, in the previous studies, the distance between the columns was not more than 8 m.

In this research, according to the previous experience of engineers, cables are added and the spans of the structures are increased. The effects of added cables on the performance of the metaheuristic algorithms to optimize the weight of the structures and mid-span deflections were investigated. Therefore, here the goal of optimization is to achieve a set of design variables that have a two-layer grid with the lowest weight, lowest cost and best performance. By adding cables to two-layer grids, larger spans can be achieved. The optimization is performed using the recent meta-heuristic algorithms by shifting the number and location of cables and their economic comparison.

This paper is organized as follows. Section 2 presents the methodology employing two metaheuristic algorithms for the optimization. Section 3 presents the results provided for the considered examples. The relative discussions and conclusions are derived in Section 4.

2 Applied methods

2.1 Methodology

In this study, SAP2000 and MATLAB software packages were used to analyze four space structures. The examples were first modeled in SAP2000 and then the optimization algorithms were coded in MATLAB. Using the connection of these two software packages, structural analysis was performed in MATLAB and in the end, the best result was obtained as the optimal weight of the structures. The applied optimization algorithms are described below (Fig. 1).

2.1.1 The ECBO algorithm

As an optimization algorithm, this paper uses the ECBO algorithm [18, 19]. The technique is based on the energy and momentum conservation law for a 1D collision, containing diverse solutions, treated as CBs (collided bodies) with defined mass and velocity. After the collision, considering the current restitution coefficient, velocity, and mass, each CB goes to a new position. The procedure of the algorithm is as follows:

Step 1: Initialization

The initial position of each CB is determined randomly (Eq. (1)):

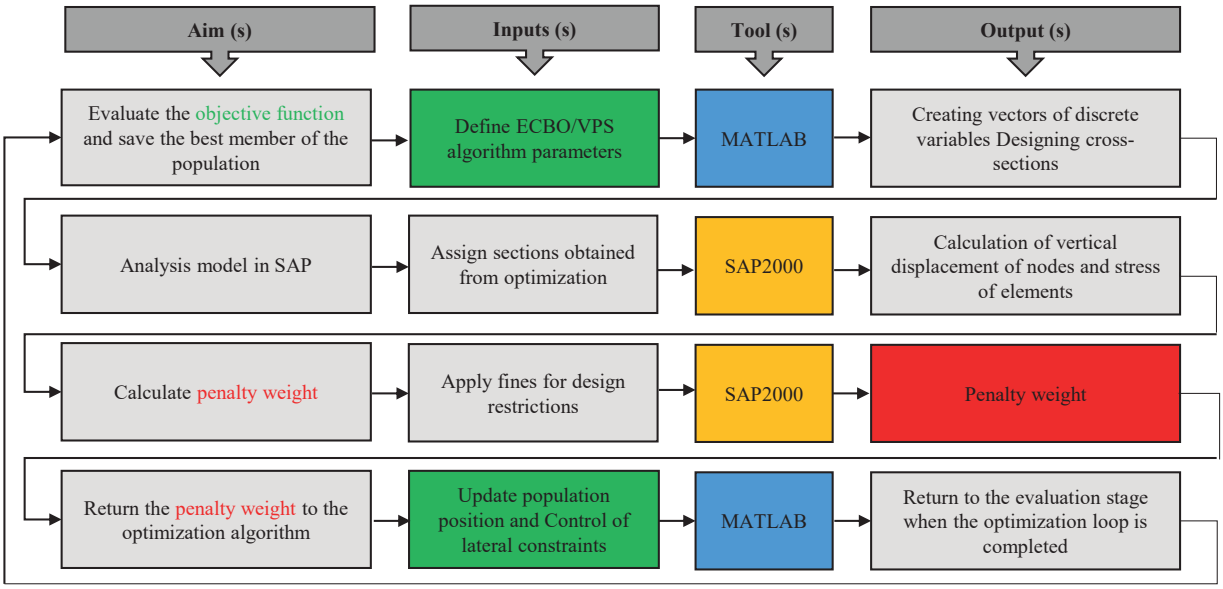

Fig. 1 The flowchart of this study

$$x_{i,j}^{0} = rand(x_{j,\max} - x_{j,\min}) + x_{j,\min},$$
$$i = 1,2,\ldots,N,\ \ j = 1,2,\ldots,n, \tag{1}$$

where $x_{i,j}^{0}$ indicates the initial value of j^{th} variable in i^{th} CB, N is the number of CBs, n is the number of variables, $x_{j,\min}$ and $x_{j,\max}$ are the lower and upper bounds, respectively, and *rand* is a random number in 0-1.

Step 2: Defining mass and fitness

The mass is assessed for each CB using Eq. (2):

$$m_i = \frac{\frac{1}{fit(i)}}{\sum_{j=1}^{N}\frac{1}{fit(j)}}, i = 1,2,3,\ldots,N, \tag{2}$$

while fit represents the objective function value of the i^{th} CB and n is the number of CBs.

Step 3: Introduction of colliding memory

The best solution is added in colliding memory and the worst CB is replaced by CBs in colliding memory.

Step 4: Update CBs

CBs are sorted by their fitness.

Step 5: Creating groups

CBs are classified into two different groups: (1) stationary group and (2) moving group. After that, CBs are matched in pairs, one chosen from the stationary and the other from the moving group.

Step 6: Initialization of velocities before collision

The velocity of stationary and moving CBs (Eq. (3) and Eq. (4), respectively) are computed by:

$$v_i = 0,\ i = 1,2,\ldots,\frac{N}{2}, \tag{3}$$

$$v_i = x_{i-\frac{N}{2}} - x_i,\ i = 1+\frac{N}{2},2+\frac{N}{2},\ldots,N, \tag{4}$$

Step 7: Updating velocities and positions

After collision, the velocities and positions of the groups (Eq. (5) and Eq. (6), respectively) is updated:

$$v'_i = \frac{(m_{i+\frac{n}{2}} + \varepsilon m_{i+\frac{n}{2}})v_{i+\frac{n}{2}}}{m_i + m_{i+\frac{n}{2}}},\ i = 1,2,\ldots,\frac{n}{2}, \tag{5}$$

$$v'_i = \frac{(m_i - \varepsilon m_{i-\frac{N}{2}})v_i}{m_i + m_{i-\frac{n}{2}}},\ i = 1+\frac{n}{2},2+\frac{n}{2},\ldots,n, \tag{6}$$

where ε is a parameter descending linearly between 0 and 1, defined as Eq. (7):

$$\varepsilon = 1 - \frac{t}{MaxDT}, \tag{7}$$

where *MaxDT* and t represent the maximum of iterations and the current iteration number, respectively. Then, Eq. (8) is applied to update the position of stationary CBs:

$$x_i^{new} = rand * v'_i + x_i,\ i = 1,2,\ldots,\frac{N}{2}, \tag{8}$$

where x_i is the previous position of the i^{th} stationary CB, x_i^{new} is its new position, v_i' is the velocity of the i^{th} CB after collision, and *rand* is a random number in [-1,1] and * illustrate the increased element by element.

Step 8: Local optimization strategy

Now, a parameter pro in 0-1 is represented to expand the local search ability. If $pro \geq rn$, one of the random variables of CB and its value is updated by Eq. (9):

$$x_{i,j} = rand * (x_{j,\max} - x_{j,\min}) + x_{j,\min},$$
$$i = 1,2,\ldots,N,\ \ j = 1,2,\ldots,n, \tag{9}$$

while $x_{i,j}$ is the value of the j^{th} variable of the i^{th} CB, $x_{j,\min}$ and $x_{j,\max}$ are the lower and upper bounds of the j^{th} variable, *rand* is a random number in 0-1, and *rn* is a random number uniformly distributed in 0-1.

Step 9: Stop

If the convergence criterion is not satisfied, Steps 2 to 8 are repeated; else, stop the process.

2.1.2 The VPS algorithm

The VPS method simulates a free vibration of single degree of freedom systems with viscous damping [20]. The VPS has a number of particles (or individuals) consisting of the variables of the problem. In the population-based algorithm, each solution candidate is defined as "X", containing a number of variables, considered as a particle. Particles are damped based on three equilibrium positions with different weights, and during each generation the position of particles are updated by: the historically best position of all particles population (*HB*), a bad particle (*BP*), and a good particle (*GP*). The candidates steadily approach to their equilibrium positions that are reached by current population and historically best position to have a proper balance between intensification and diversification. The algorithm contains the following steps:

Step 1: Initialization

Initial locations of particles are created randomly in an n-dimensional search space by Eq. (10):

$$x_j^i = rand(\boldsymbol{x}_{\max} - \boldsymbol{x}_{\min}) + x_{\min},\ i = 1,2,\ldots,N, \tag{10}$$

while x_i^j is the j^{th} variable of the i^{th} particle. In addition, $\boldsymbol{x}_{max}$ and $\boldsymbol{x}_{min}$ are respectively the minimum and the maximum allowable values vector of variables. And *rand* is a random number in the interval [0,1]; and *n* is the number of particles.

Step 2: Assessment of candidate solutions and updating the particle positions

The objective function is computed for each particle and to choose the GP and BP for each candidate solution, the current population is sorted according to their objective function values in an increasing order, and then GP and BP are selected randomly from the first and second half, respectively. So, the particle's position can be updated by Eq. (11):

$$x_j^i = \omega_1[DF * k * R_1 + HB^j] + \omega_2[DF * k * R_2 + GP^j] + \omega_3[DF * k * R_3 + BP^j], \quad (11)$$

while x_i^j is the j^{th} variable of the particle *i*. ω_1, ω_2 and ω_3 are three parameters to measure the relative importance of *HB*, *GP* and *BP,* respectively ($\omega_1 + \omega_2 + \omega_3 = 1$). R_1, R_2, and R_3 are uniformly distributed random numbers between 0 and 1, respectively. And *k* is defined as:

$$k = [\omega_1(HB^j - x_j^i)] + [\omega_1(GP^j - x_j^i)] + [\omega_1(BP^j - x_j^i)]. \quad (12)$$

Parameter DF is a descending function based on the number of iterations:

$$DF = \left(\frac{iter}{iter_{max}}\right)^{-\alpha}. \quad (13)$$

In order to have a fast convergence in the VPS, the effect of *BP* is sometimes considered in updating the position formula. So, for each particle, parameter *p* in the range of (0,1) is defined, and it is compared to rand (a randomly chosen number, uniformly distributed between 0 and 1) and if $p < rand$, then $\omega_3 = 0$.

Particles go towards *HB* so the self-adaptation is provided. Each particle has the chance to have the influence on the new position of the other one, so the cooperation between the particles is provided. Because of the parameter *p*, the influence of *GP* is more than that of *BP*, and thus, a completion is established.

Step 3: Handling the side constraints

There is a likelihood of boundary violation when a particle goes to a new position. In the present technique, for handling boundary constraints a harmony search-based algorithm is utilized. In this approach, there is a probability like harmony memory considering rate that specifies whether the violating component has to be changed with the corresponding component of the historically best position of a random particle or it must be determined randomly in the search space. Furthermore, if the component of a historically best position is chosen, there is a probability like pitch adjusting rate that specifies whether this value must be changed with the neighboring value or not.

Step 4: Terminating condition check

Steps 2–3 are repeated until a termination criterion is fulfilled. And each terminating condition may be considered.

Further explanations and many recently developed meta-heuristic algorithms and their applications can be found in [21–25].

2.2 Pattern models

In this study, design optimization of four double-layer grid roof structures, with different spans with and without cables, were investigated. The examples included the following:

Example 1: A 2816-bar double-layer grid, larger square on square, with 16 meter-spanning: Fig. 2(a) shows a schematic of the analyzed structure. It consists of two symmetrical sections of 1408 members and 380 nodes, located 2 m apart. As shown in the figure, the supports are located in the bottom layer with a distance of 16 m from each other. A16 kN force is applied to each node in the upper layer of concentrated force. The cross-sectional area is divided into 27 groups.

Example 2: A 2842-bar double-layer grid with cables, larger square on square, with 16 meter-spanning: Fig. 2(b) shows a schematic of the analyzed structure. It consists of a 2816-member flat two-layer grid and 2 towers with a square cross-section and 24 cables, each of which is supported by 12 cables connected from the top of each tower to the top layer of the two-layer grid.

Example 3: A 2816-bar double-layer grid, larger square on square, with 32 meter-spanning: Fig. 2(c) shows a schematic of the analyzed structure. 2816-member flat two-layer grid consists of two symmetrical parts of 1408 members and 380 nodes with dimensions of 44x64 square meters, which are located at a distance of 2 m from each other. The supports are located in the bottom layer with a distance of 32 m from each other as shown in the figure.

Example 4: A 2842-bar double-layer grid with cables, larger square on square, with 32 meter-spanning: Fig. 2(d) shows a schematic of the analyzed structure. It consists of a 2816-member flat two-layer grid and 2 towers with a square cross-section of 39 meters and 24 cables, each of which is supported by 12 cables that are connected to the top layer of the two-layer grid from the top of each tower.

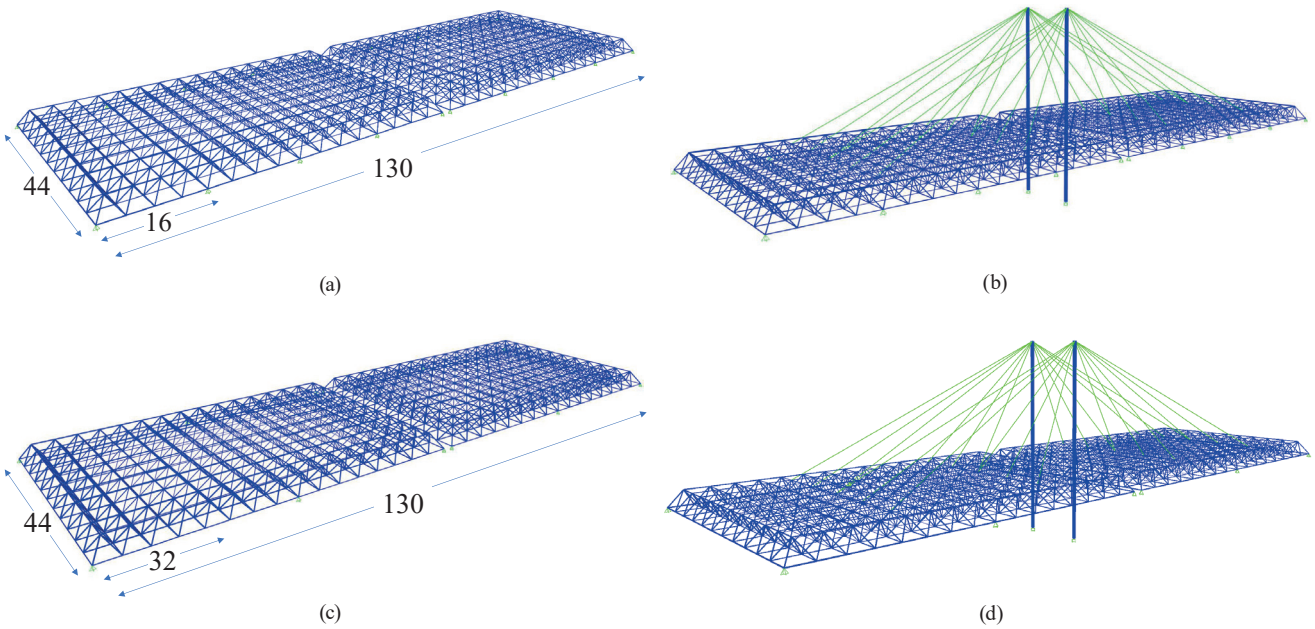

Fig. 2 (a) Example 1, (b) Example 2, (c) Example 3, (d) Example 4

A dimension of 44 × 64 m^2 and the height of 3 m were considered for the examples. Also, all of the connections were assumed to be ball jointed. The design variables were the cross-sectional areas of the bar elements, chosen from the list of steel pipe sections from AISC-LRFD (Table 1). The density of steel, the modulus of elasticity, and the yield stress were taken as 7833.413 kg/m^3, 205 GPa, and 248.2 MPa, respectively. Strength and slenderness limitations were according to AISC-LRFD provisions and displacement limitations of span/600 were imposed on all nodes in the vertical direction. In addition, different types of the used cables are shown in Table 2. The cables are made of two steel towers with a hollow square cross section with a wall thickness of 5 cm and a height of 39 m, with ASTM-A572 (G50) standard with a modulus of elasticity of 205 GPa and a density of 78490 kg/m^3. The height of the lower layer of the roof from the ground is 12 m and from the upper layer to the top of the towers is 24 m. The cables used in these examples are stranded cables (strands) made of stainless steel with ASTM-A416 standard with a modulus of elasticity of 196 GPa and a density of 7849 kg/m^3. Each example has been solved 10 times independently, and 1000 iterations were considered as the terminal condition. A population of 20 particles was considered for each algorithm and the other algorithm parameters were set. The optimization algorithms were coded in MATLAB and the structures were analyzed, using the direct stiffness method by our own codes.

3 Design and discussion

3.1 Optimal section design by the ECBO and VPS algorithms

In order to compare the performance of the applied ECBO and VPS algorithms, Tables 3 and 4 provide a list of optimal sections of the algorithms for the pattern models. As the tables indicate, in general, the ECBO algorithm gives the lightest weight of the structure compared to the VPS method.

Figs. 4 to 7 offer more detailed information about the results of the node displacement diagrams, and the convergence curves of the analyzed model for the best answer for Examples 1 to 4.

In this model, significant displacement of the nodes is in the middle of each side roof, and the results of the analysis of the VPS algorithm started to being converged earlier and after iteration number 6000 the results of the both algorithms were very close to each other. Finally, the ECBO algorithm gives the best results compared to the VPS method, in the span allowable displacement.

In this model, with the addition of cables, the rise in the middle of the opening was reduced. In this model, the VPS algorithm converged earlier and after repeating number 6000, the answers were very close to each other, but in the end, the most optimal answer was obtained by the ECBO algorithm.

In this example, the results of the analysis were converged earlier with the VPS algorithm, and the jobs of the

Table 1 The steel pipe sections

Number	Type	Nominal diameter (in)	Label	Area (cm^2)	Gyration radius (cm)
1	ST[a]	½	P 0.5	1.6129	0.662432
2	EST[b]	½	XP 0.5	2.064512	0.635
3	ST	¾	P 0.75	2.129028	0.846582
4	EST	¾	XP 0.75	2.774188	0.818896
5	ST	1	P 1	3.161284	1.066038
6	EST	1	XP 1	4.129024	1.034542
7	ST	1 ¼	P 1.25	4.322572	1.371346
8	ST	1 ½	P 1.5	5.16128	1.582166
9	EST	1 ¼	XP 1.25	5.677408	1.331214
10	EST	1 ½	XP 1.5	6.903212	2.003806
11	ST	2	P 2	6.903212	1.53543
12	EST	2	XP 2	9.548368	1.945132
13	ST	2 ½	P 2.5	10.96772	2.41681
14	ST	3	P 3	14.387068	2.955798
15	EST	2 ½	XP 2.5	14.5161	2.345462
16	DEST[c]	2	XXP 2	17.161256	1.782572
17	ST	3 ½	P 3.5	17.290288	3.395726
18	EST	3	XP 3	19.483832	2.882646
19	ST	4	P 4	20.451572	3.835908
20	EST	3 ½	XP 3.5	23.741888	3.318002
21	DEST	2 ½	XXP 2.5	25.999948	2.143506
22	ST	5	P 5	27.74188	4.775454
23	EST	4	XP 4	28.45155	3.749548
24	DEST	3	XXP 3	35.290252	2.65811
25	ST	6	P 6	35.999928	5.700014
26	EST	5	XP 5	39.419276	4.675124
27	DEST	4	XXP 4	52.25796	3.490976
28	ST	8	P 8	54.19344	7.462012
29	EST	6	XP 6	54.19344	5.577332
30	DEST	5	XXP 5	72.90308	4.379976
31	ST	10	P 10	76.77404	9.342628
32	EST	8	XP 8	82.58048	7.309358
33	ST	12	P 12	94.19336	11.10361
34	DEST	6	XXP 6	100.64496	5.236464
35	EST	10	XP 10	103.87076	9.216898
36	EST	12	XP 12	123.87072	11.028934
37	DEST	8	XXP 8	137.41908	7.004812

a ST: standard weight,
b EST: extra strong
c DEST: double-extra strong

Table 2 List of cable sections used in modelling

Number	Nominal diameter (in)	Area (mm^2)	Moment of inertia (mm^4)	Torsion factor (mm^4)
CAB 1	3	4560.37	1654968.7	3309937.4
CAB 2	4	8107.32	5230518.36	10461036.71
CAB 3	5	12667.69	12769820.2	25539640.41

two algorithms became very close after repeating the number 15000, but in the end, the best answer was obtained by the ECBO algorithm.

In this model, with the addition of cables, the rise in the middle of the opening was reduced, but the results of the analysis were converged with the ECBO algorithm sooner. The answers of both algorithms became very close after repeating the number 4000. Finally, the most optimal answer was obtained by the ECBO algorithm in the allowable range in the middle of the opening.

3.2 Discussion of the results

In this study, aligned with previous studies, the dimensions of the structure were considered larger: the distance between the columns was increased from 8 meters to 16 and 32 meters. The cable was used as an intermediate support to examine the use of the structure for use as an aircraft hangar. The results of this study are in line with previous research conducted on two-layer grids. Considering that the comparison of algorithms in optimizing different types of two-layer grids had been previously studied by Kaveh and Ilchi Ghazaan [26], the two algorithms that had the best answers and the least standard deviation were considered to optimise the example models.

In all examples, the best weight was obtained by the ECBO algorithm. In Example 2, the weight of the structure was 167711.9 kg, which was about 36 tons lighter than the cable-less model. In example 4, the weight of the structure was 178799.96 kg, which was about 72 tons lighter than the cable-less model. In all examples, cables with a diameter of 3 inch were selected as the most optimal cross-section for cables, with a total weight of 24 cables of 36325.36 kg. The weight of the two towers was calculated to be 55100.31 kg. The weight of the roof with cable decreased by about 18% compared to the roof without cable when the column spacing was 16 m. The number changed to 28% when the column spacing was 32 m. None of the designed sections obtained by the algorithms exceeded the allowable range of design constraints. In addition to reducing the weight of the roof, the cables also reduced the maximum span of the middle span and in Example 2, the maximum rise in the middle of the span was less than 6.5 cm and in example 4, less than 5.5 cm, which is about 1 and 2 cm lower than the allowable rise of the cable-free model, respectively.

It should be noted that the purpose of optimization is to find the answer that is close to the optimal, so it cannot be claimed that the obtained answer is necessarily the most

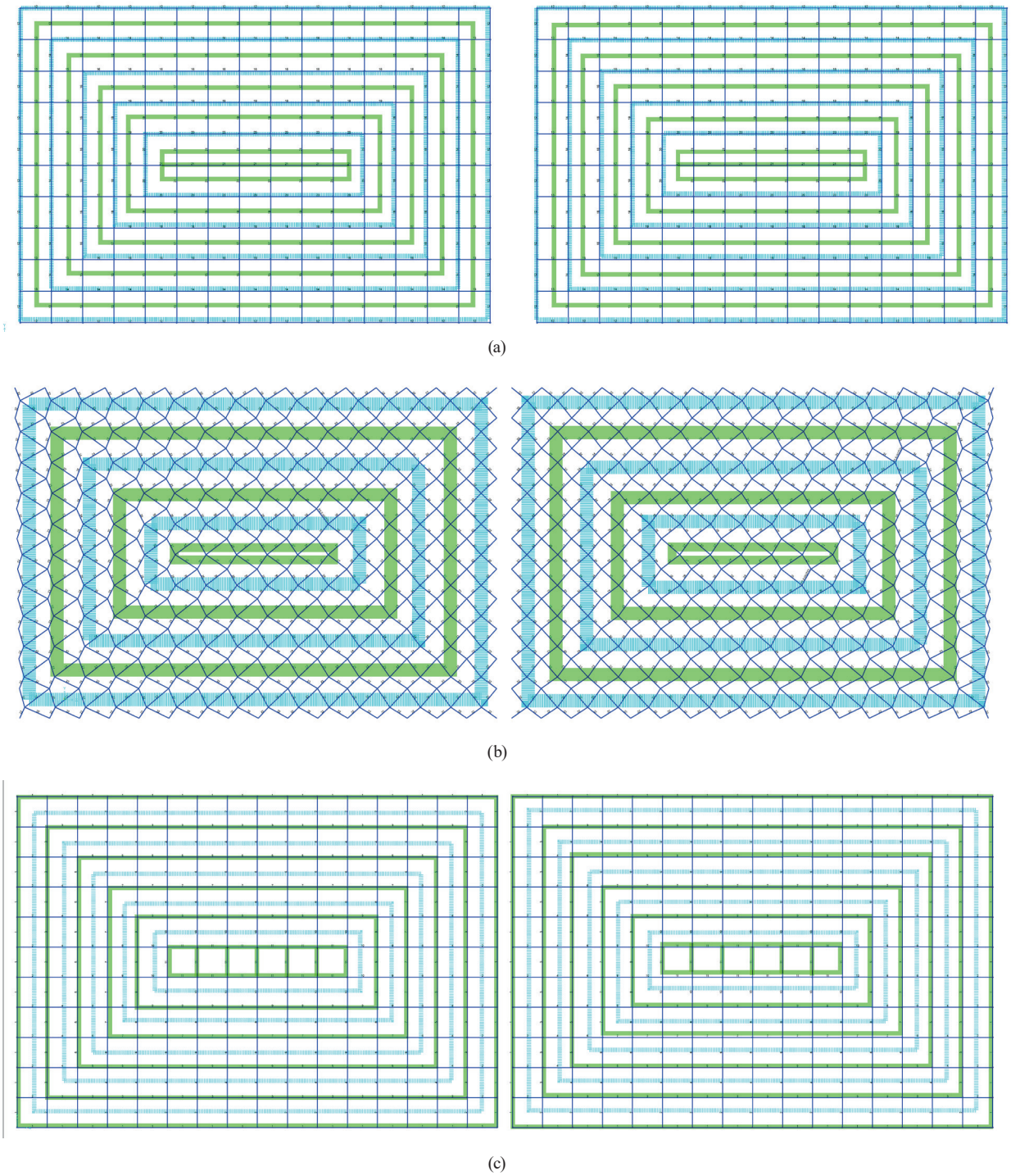

Fig. 3 Grouping roof grid layers: (a) the top layer, from the outside to the inside of the green grid, respectively: group numbers: 21, 19, 17, 15, 13. And from the outside to the inside of the blue grid, respectively: group numbers: 18, 16, 14, 12, 20. (b) the middle layer, from the outside to the inside of the green grid, respectively: group numbers: 27, 25, 23. And from the outside to the inside of the blue grid, respectively: group numbers: 26, 24, 22. And (c) the bottom layer, from the outside to the inside of the green grid, respectively: group numbers: 5, 3, 1, 11, 9, 7. And from the outside to the inside of the blue grid, respectively: group numbers: 10, 8, 6, 4, 2.

optimal one. Given that the dimensions of the optimized structure were much larger than the previous examples and the time of each analysis was much longer, and each example was analyzed 20,000 times and this operation was performed 10 times separately for each example, it is possible to obtain more optimal answers than the obtained values by increasing the number of population and search space of the algorithm and solving the problem with more numbers.

Table 3 Comparison list of optimal sections of the used algorithms for the pattern models

Group number	Example 1		Example 2		Example 3		Example 4	
	ECBO	VPS	ECBO	VPS	ECBO	VPS	ECBO	VPS
1	ST 5	ST 3 ½	ST 3 ½	ST 4	EST 4	ST 5	ST 6	EST 3 ½
2	ST 5	ST 6	ST 3 ½	ST 3 ½	ST 5	ST 8	ST 3 ½	ST 3 ½
3	ST 2 ½	ST 8	DEST 2 ½	EST 3	ST 6	ST 4	ST 3	ST 3 ½
4	ST 3	ST 3 ½	ST 3 ½	EST 1 ½	ST 3 ½	ST 4	EST 1 ½	ST 2 ½
5	EST 1 ½	ST 3	EST 3	ST 2 ½	ST 2 ½	ST 3	EST 1 ½	EST 2 ½
6	DEST 2	ST 2 ½	ST 2 ½	ST 2 ½	EST 3 ½	ST 3	ST 2 ½	ST 3
7	EST 3	ST 2 ½	ST 4	ST 3	ST 2 ½	EST 1 ½	ST 3	DEST 3
8	ST 4	EST 2	ST 3	ST 3	DEST 4	ST 3	ST 3	EST 3 ½
9	ST 2 ½	ST 2	ST 3	EST 3	ST 3	EST 1 ½	ST 3 ½	EST 5
10	ST 4	ST 2 ½	ST 5	ST 4	ST 8	DEST 3	ST 4	EST 3 ½
11	EST 2	ST3	ST 3	ST 3	DEST 3	ST 6	ST 3	EST 3
12	ST 5	ST 5	ST 8	EST 5	ST 6	ST 6	DEST 5	ST 5
13	ST 5	ST 5	ST 3	ST 3 ½	ST 6	ST 6	ST 3 ½	ST 3 ½
14	ST 6	EST 4	ST 4	ST 3 ½	ST 6	ST 6	ST 3	ST 5
15	ST 6	ST 5	ST 4	ST 3 ½	EST 5	EST 6	ST 4	ST 3 ½
16	ST 6	EST 4	ST 3 ½	ST 4	ST 8	EST 5	ST 2 ½	ST 6
17	ST 5	EST 6	ST 4	ST 3 ½	ST 6	DEST 4	ST 5	ST 3 ½
18	ST 4	ST 5	ST 3 ½	ST 3 ½	ST 5	EST 4	ST 3 ½	ST 4
19	ST 6	ST 5	ST 4	ST 5	ST 6	ST 6	EST 4	EST 3 ½
20	EST 4	ST 5	ST 5	DEST 3	ST 5	ST 5	ST 3 ½	ST 5
21	ST 5	ST 5	ST 3 ½	ST 6	EST 5	EST 5	ST 4	EST 3
22	ST 5	ST 5	ST 4	EST 4	ST 6	ST 6	ST 5	ST 5
23	ST 5	ST 5	ST 3	ST 3 ½	ST 6	ST 6	ST 3 ½	EST 3
24	ST 3 ½	ST 3 ½	ST 3	ST 3	ST 3 ½	ST 5	ST 3	ST 3
25	ST 2 ½	ST 2 ½	ST 3	ST 3	ST 2 ½	ST 2 ½	ST 3	ST 3
26	ST 2 ½	ST 2 ½	ST 2 ½	ST 2 ½	ST 2 ½	ST 2 ½	ST 2 ½	ST 2 ½
27	ST 2 ½	ST 2 ½	ST 3	ST 3	ST 2 ½	ST 2 ½	ST 3 ½	ST 3

Table 4 Comparison list of the performance of the used algorithms

Parameter	Example 1		Example 2		Example 3		Example 4	
	ECBO	VPS	ECBO	VPS	ECBO	VPS	ECBO	VPS
Weight (Kg)	199958.2	204522.4	164711.9	170153.8	250587.4	256758.2	178800.0	181862.9
Average optimised weight (Kg)	205898.8	212724.8	171882	178123.9	259180	265805.9	186854	197428.9
Max ratio (%)	99.63	93.74	94.85	92.70	95.14	97.20	94.92	96.02
Standard deviation on average weight	5563	4969	6107	6016	5325	4797	7031	7218

4 Conclusions

The purpose of this study was to investigate the effects of cables on optimizing the weight of two-layer grids and its economic justification. According to the results, in addition to lightening the structural weight of the cables in the middle of the opening, the cables also reduce the weight. But the impact of the cable became apparent when the distance between the columns along the grid was increased from 16 m to 32 m. In fact, when the distance between the columns was 16 m and 32 m, the minimum weight obtained was reduced by about 18% and about 28%, respectively, compared to the cable less model.

However, is it economical to use two-layer grids with cables or not? Due to the fact that the use of cables can reduce the number of columns, in addition to saving materials over time, the cost of maintenance of the structure is also reduced. The structure of the studied models is such that the number of cables and masts to which the roofs are connected

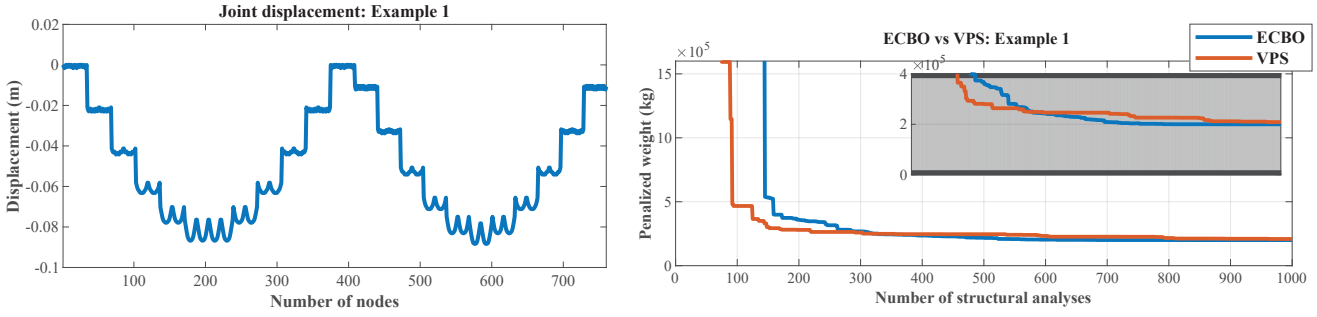

(a) (b)

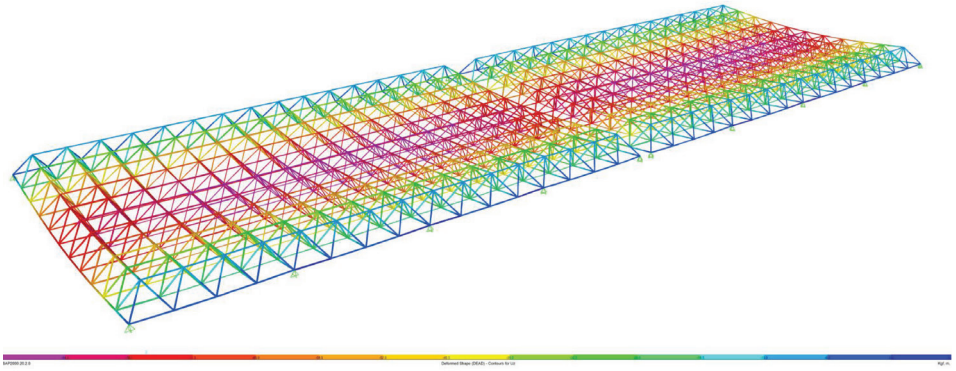

(c)

Fig. 4 Example 1 (a) the node displacement diagram, (b) the convergence curve, and (c) the deformed shape of the analyzed model under the load for the best answer

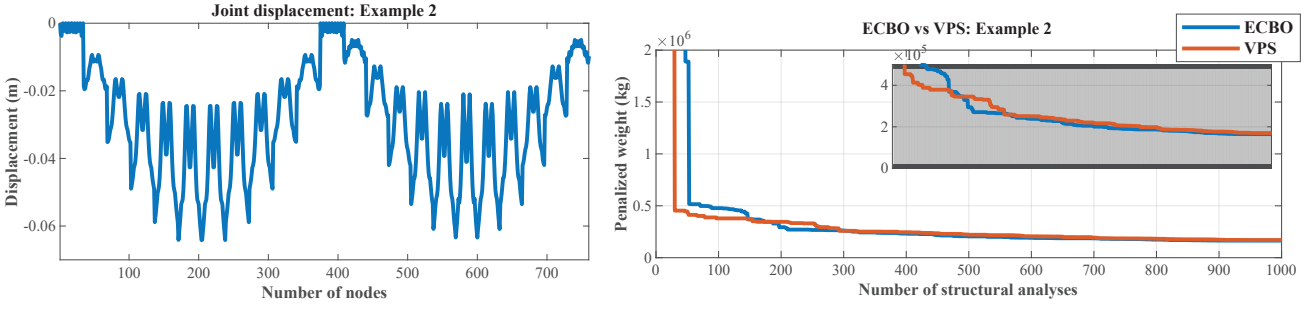

(a) (b)

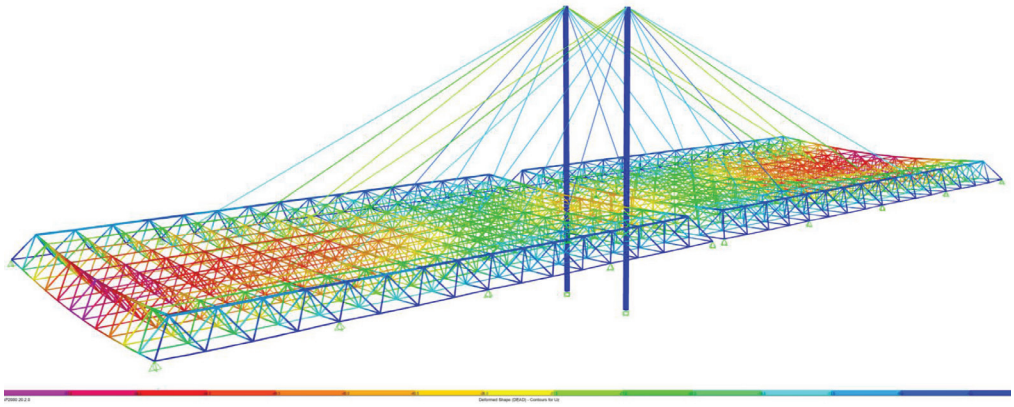

(c)

Fig. 5 Example 2 (a) the node displacement diagram, (b) the convergence curve, and (c) the deformed shape of the analyzed model under the load for the best answer

is also saved. The use of two-layer grids with cables allows the roof to be implemented horizontally as much as possible in large areas such as gyms, instead of structures such as sheds, which will significantly reduce the cost of energy used for heating and cooling inside the structure.

Among the benefits of cables are the following: (1) net tensile behavior due to adaptation to the natural flow of forces and deformation with any new loading condition, (2) can be used in large openings, (3) have better interior performance for large spaces without columns, (4) the lightness of the structure, which leads to high resistance to earthquakes, (5) high speed in installing and dismantling structures that are suitable for temporary operations, and (6) the use of fewer materials due to their weight-to-span ratio makes them the most economical system for covering spaces with large spans.

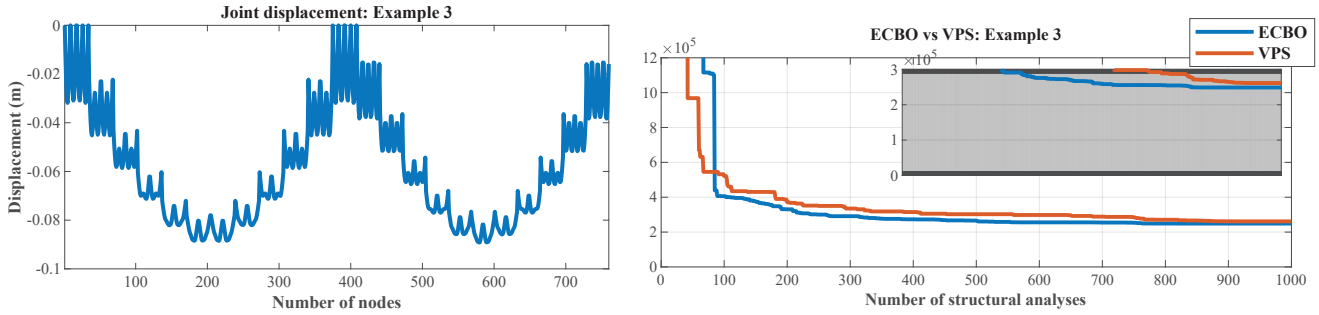

(a) (b)

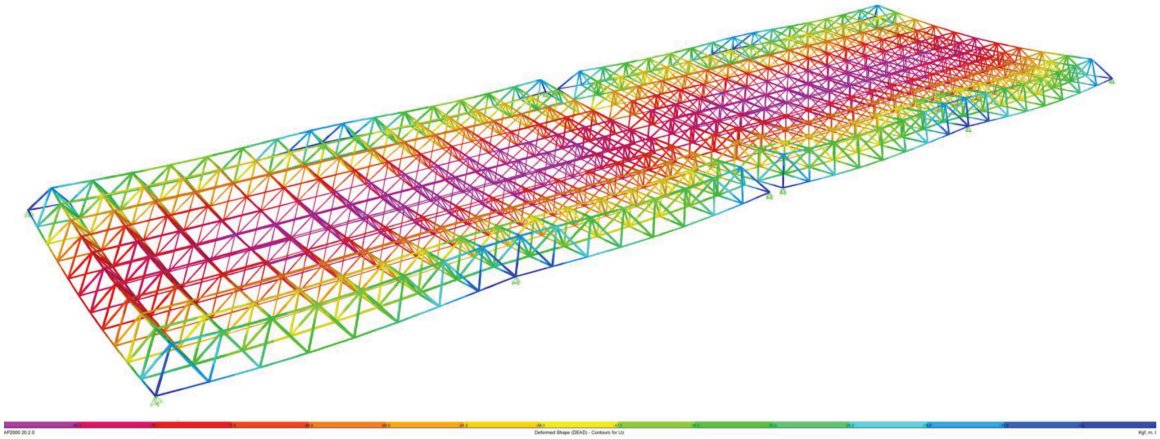

(c)

Fig. 6 Example 3 (a) the node displacement diagram, (b) the convergence curve, and (c) the deformed shape of the analyzed model under the load for the best answer

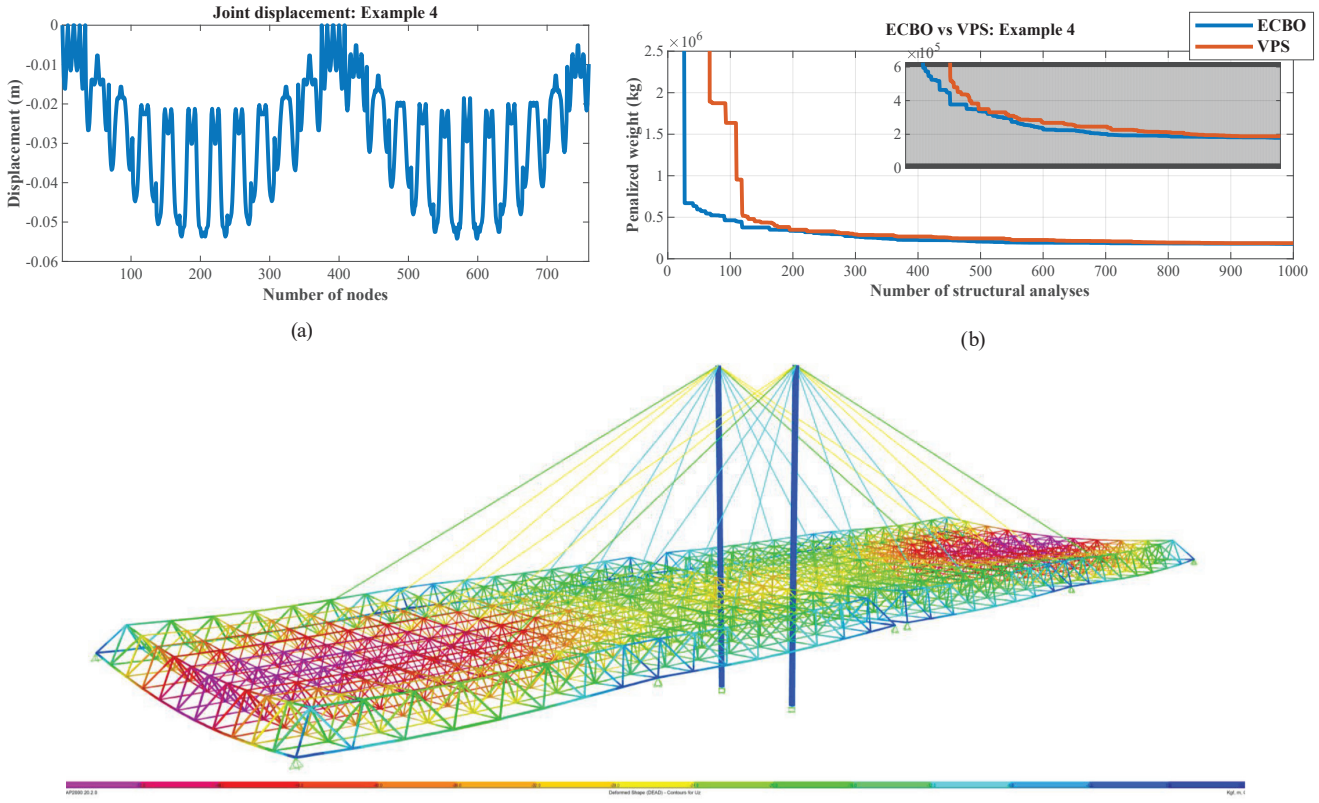

Fig. 7 Example 4 (a) the node displacement diagram, (b) the convergence curve, and (c) the deformed shape of the analyzed model under the load for the best answer

References

[1] Kaveh, A. "Advances in Metaheuristic Algorithms for Optimal Design of Structures", 3rd ed., Springer, 2021. ISBN: 978-3-030-59391-9
https://doi.org/10.1007/978-3-030-59392-6

[2] Ye, J. "An improved neutrosophic number optimization method for optimal design of truss structures", New Mathematics and Natural Computation, 14(3), pp. 295–305, 2018.
https://doi.org/10.1142/S1793005718500187

[3] Kaveh, A., Hoseini Vaez, S. R., Hosseini, P., Bakhtyari, M. "Optimal Design of Steel Curved Roof Frames by Enhanced Vibrating Particles System Algorithm", Periodica Polytechnica Civil Engineering, 63(4), pp. 947–960, 2019.
https://doi.org/10.3311/PPci.14812

[4] Wang, D., Xu, W. "Minimum Weight Optimal Design of Truss Structure with Frequency Response Function Constraint", Journal of Aerospace Engineering, 33(4), 04020028, 2020.
https://doi.org/10.1061/(ASCE)AS.1943-5525.0001149

[5] Sonmez, M. "Performance Comparison of Metaheuristic Algorithms for the Optimal Design of Space Trusses", Arabian Journal for Science and Engineering, 43, pp. 5265–5281, 2018.
https://doi.org/10.1007/s13369-018-3080-y

[6] Jawad, F. K. J., Mahmood, M., Wang, D., Al-Azzawi, O., Al-Jamely, A. "Heuristic dragonfly algorithm for optimal design of truss structures with discrete variables", Structures, 29, pp. 843–862, 2021.
https://doi.org/10.1016/j.istruc.2020.11.071

[7] Karoki Kabando, E., Gong, J. "An overview of long-span spatial grid structures failure case studies", Asian Journal of Civil Engineering, 20, pp. 1137–1152, 2019.
https://doi.org/10.1007/s42107-019-00168-4

[8] Vinothni, S. N., Sangeetha, P. "Space Frame Structure as Roof and Floor System – A Review", In: Sustainable Practices and Innovations in Civil Engineering, Springer, 2022, pp. 291–298. ISBN: 978-981-16-5040-6
https://doi.org/10.1007/978-981-16-5041-3_22

[9] Zhang, C., Nie, G., Dai, J., Zhi, X. "Experimental studies of the seismic behavior of double-layer lattice space structures I: Experimental verification", Engineering Failure Analysis, 64, pp. 83–96, 2016.
https://doi.org/10.1016/j.engfailanal.2016.03.002

[10] Helou, M., Kara, S. "Design, analysis and manufacturing of lattice structures: an overview", International Journal of Computer Integrated Manufacturing, 31(3), pp. 243–261, 2018.
https://doi.org/10.1080/0951192X.2017.1407456

[11] Nie, G., Zhang, C., Dai, J., Liu, K. "Seismic Damage Investigation and Seismic Performance Study of Space Double-Layered Lattice Structure", Journal of Performance of Constructed Facilities, 32(2), 04018003, 2018.
https://doi.org/10.1061/(ASCE)CF.1943-5509.0001144

[12] Adil, B., Cengiz, B. "Optimal design of truss structures using weighted superposition attraction algorithm", Engineering with Computers, 36, pp. 965–979, 2020.
https://doi.org/10.1007/s00366-019-00744-x

[13] Nooshin, H. "Formex configuration processing: A young branch of knowledge", International Journal of Space Structures, 32(3–4), pp. 136–148, 2017.
https://doi.org/10.1177/0266351117736968

[14] Kaveh, A., Ilchi Ghazaan, M. "Vibrating particles system algorithm for truss optimization with multiple natural frequency constraints", Acta Mechanica, 228, pp. 307–322, 2017.
https://doi.org/10.1007/s00707-016-1725-z

[15] Jafari, M., Salajegheh, E., Salajegheh, J. "Optimal design of truss structures using a hybrid method based on particle swarm optimizer and cultural algorithm", Structures, 32, pp. 391–405, 2021.
https://doi.org/10.1016/j.istruc.2021.03.017

[16] Kaveh, A., Ilchi Ghazaan, M., Saadatmand, F. "Colliding bodies optimization with Morlet wavelet mutation and quadratic interpolation for global optimization problems", Engineering with Computers, 38, pp. 2743–2767, 2022.
https://doi.org/10.1007/s00366-020-01236-z

[17] Movahedi Rad, M., Habashneh, M., Lógó, J. "Elasto-plastic limit analysis of reliability based geometrically nonlinear bi-directional evolutionary topology optimization", Structures, 34, pp. 1720–1733, 2021.
https://doi.org/10.1016/j.istruc.2021.08.105

[18] Kaveh, A., Mahdavi, V. R. "Colliding Bodies Optimization", Springer, 2015. ISBN: 978-3-319-19658-9
https://doi.org/10.1007/978-3-319-19659-6

[19] Kaveh, A., Kamalinejad, M., Arzani, H., Barzinpour, F. "New enhanced colliding body optimization algorithm based on a novel strategy for exploration", Journal of Building Engineering, 43, 102553, 2021.
https://doi.org/10.1016/j.jobe.2021.102553

[20] Kaveh, A., Ilchi Ghazaan, M. "A new meta-heuristic algorithm: vibrating particles system", Scientia Iranica, 24(2), pp. 551–566, 2017.
https://doi.org/10.24200/sci.2017.2417

[21] Kaveh, A., Zolghadr, A. "Topology optimization of trusses considering static and dynamic constraints using the CSS", Applied Soft Computing, 13(5), pp. 2727–2734. 2013.
https://doi.org/10.1016/j.asoc.2012.11.014

[22] Kaveh, A., Biabani Hamedani, K., Hosseini, S. M., Bakhshpoori, T. "Optimal design of planar steel frame structures utilizing meta-heuristic optimization algorithms", Structures, 25, pp. 335–346, 2020.
https://doi.org/10.1016/j.istruc.2020.03.032

[23] Kaveh, A., Hoseini Vaez, S. R., Hosseini, P., Fathali, M. A. "Heuristic Operator for Reliability Assessment of Frame Structures", Periodica Polytechnica Civil Engineering, 65(3), pp. 702–716, 2021.
https://doi.org/10.3311/PPci.17580

[24] Lógó, J., Movahedi Rad, M., Knabel, J., Tauzowski, P. "Reliability based design of frames with limited residual strain energy capacity", Periodica Polytechnica Civil Engineering, 55(1), pp. 13–20, 2011.
https://doi.org/10.3311/pp.ci.2011-1.02

[25] Habashneh, M., Rad, M. M. "Reliability based geometrically nonlinear bi-directional evolutionary structural optimization of elasto-plastic material", Scientific Reports, 12, 5989, 2022.
https://doi.org/10.1038/s41598-022-09612-z

[26] Kaveh, A., Ilchi Ghazaan, M. "Optimal design of double-layer grids", In: Meta-heuristic algorithms for optimal design of real-size structures, Springer, 2018, pp. 65–83. ISBN: 978-3-319-78779-4
https://doi.org/10.1007/978-3-319-78780-0_5